DNA Annealing Mediated by Rad52 and Rad59 Proteins[*]

Yun Wu, Tomohiko Sugiyama[1]**, and Stephen C. Kowalczykowski**[2]

*From the Sections of Microbiology and Molecular and Cellular Biology, Center for Genetics and Development,
Division of Biological Sciences, University of California, Davis, California 95616-8665*

In the budding yeast *Saccharomyces cerevisiae*, the *RAD52* gene is essential for all homologous recombination events and its homologue, the *RAD59* gene, is important for those that occur independently of *RAD51*. Both Rad52 and Rad59 proteins can anneal complementary single-stranded (ss) DNA. We quantitatively examined the ssDNA annealing activity of Rad52 and Rad59 proteins and found significant differences in their biochemical properties. First, and most importantly, they differ in their ability to anneal ssDNA that is complexed with replication protein A (RPA). Rad52 can anneal an RPA-ssDNA complex, but Rad59 cannot. Second, Rad59-promoted DNA annealing follows first-order reaction kinetics, whereas Rad52-promoted annealing follows second-order reaction kinetics. Last, Rad59 enhances Rad52-mediated DNA annealing at increased NaCl concentrations, both in the absence and presence of RPA. These results suggest that Rad59 performs different functions in the recombination process, and should be more accurately viewed as a Rad52 paralogue.

Repair of DNA double-strand breaks (DSBs)[3] is a crucial process needed to maintain cell viability and genomic integrity. An unrepaired DSB can result in growth arrest, loss of genetic information, or cell death (1). In *Saccharomyces cerevisiae*, genes in the *RAD52* epistasis group are responsible for homologous recombination-dependent DSB repair (2–4). To repair a DSB, the DNA end is first processed to reveal a 3′ single-stranded (ssDNA) tail, which is subsequently channeled into one of the recombinational pathways. The canonical gene conversion pathway is an evolutionarily conserved process carried out by the DNA strand exchange protein, Rad51 (5). Genes that are important for the gene conversion pathways are *RAD51*, *RAD52*, *RAD54*, *RAD55*, *RAD57*, and *RFA1*, which collectively define the *RAD51*-dependent recombination pathway (2, 4).

In addition to the *RAD51*-dependent recombination, alternative repair pathways exist that are independent of *RAD51* function. These pathways have different but overlapping genetic requirements from the classical gene conversion pathway (1, 6–8). In *S. cerevisiae*, the major *RAD51*-independent pathway is single-stranded annealing (SSA). The SSA pathway does not involve Rad51-mediated invasion of dsDNA and the subsequent strand exchange steps. Instead, it occurs by annealing of complementary ssDNA on either side of the DSB, followed by removal of heterologous tails and ligation of the nicks (2). In addition to the

recombination genes *MRE11*, *RAD50*, *XRS2*, *RAD52*, and *RAD59* (6, 7), the SSA pathway also depends on the *MSH2*, *MSH3* (7, 9), *RAD1* and *RAD10* (9, 10) genes. SSA in yeast is highly effective, accounting for 35–80% of DSB repair events when a DSB occurs between two direct repeats (2, 6, 11).

The *RAD52* gene encodes a 471-residue protein that is required for all homologous recombination events in *S. cerevisiae* (2, 4). The ~200-residue N terminus of Rad52 protein is highly conserved in most eukaryotic species; whereas the C terminus confers species-specific interaction with Rad51 protein (12, 13). Purified yeast and human Rad52 proteins form a multimeric ring structure (14–17), bind to ssDNA and dsDNA, anneal complementary ssDNA in the absence (18, 19) or presence (16, 20) of replication protein A (RPA) from the same species, and alleviate the inhibitory effect of RPA in Rad51-mediated DNA strand exchange (21–25).

Rad59 protein is a smaller, 238-residue protein with homology to the N terminus of Rad52 protein, a domain that is important in DNA binding and annealing. Although Rad52 protein is found in most eukaryotes, Rad59 has only been identified in fungal species, including *S. cerevisiae* (26) and *Kluyveromyces lactis* (27). Rad59 proteins from different species bear higher sequence similarity to each other than to the Rad52 protein from the same species. In *S. cerevisiae*, cells defective in *RAD59* show decreased or delayed recombination between inverted repeat sequences (26, 28) and SSA (7, 29, 30). Mutation of both *RAD51* and *RAD59* produces a synergistic reduction in recombination (26, 31), suggesting competition between these two modes of DNA repair. Rad59 protein interacts with Rad52 protein *in vivo* (29, 32), consistent with the genetic findings that the collaboration of Rad52 and Rad59 proteins is required for the *RAD51*-independent pathways. Purified Rad59 protein binds ssDNA preferentially over dsDNA, and anneals complementary ssDNA (29, 33).

Although there have been reports characterizing the biochemical activities of Rad59 protein (29, 33), the functional differences between Rad52 and Rad59 proteins have not yet been clearly resolved. Here, we provide a quantitative comparison of the yeast Rad52 and Rad59 proteins with respect to their biochemical activities. We find that despite their similar ability to anneal complementary ssDNA, these two proteins differ in significant respects. Perhaps most importantly with the regard to their biological function, they differ in their capacity to anneal complementary ssDNA that is bound by RPA. In contrast to a previous report (29), we find that Rad59 protein cannot anneal complementary ssDNA-RPA complexes although Rad52 protein can. We see no additive or synergistic effect in DNA annealing when both proteins are present at optimal reaction conditions. However, Rad59 protein increases the resistance of Rad52-dependent annealing to inhibition by NaCl, suggesting that Rad59 protein stabilizes the Rad52-ssDNA complex. Finally, the kinetic mechanism of DNA annealing by these two proteins is different, further underscoring their uniqueness. Due to their dissimilar genetic and biochemical properties, we propose that Rad59 should be designated as a "Rad52 paralogue," which plays an accessory role in

[1] Current address: Dept. of Biological Sciences, 211 Life Sciences Research Facility, Ohio University, Athens, OH 45701.
[2] To whom correspondence should be addressed: Briggs Hall, One Shields Ave., Davis, CA 95616-8665. Tel.: 530-752-5938; Fax: 530-752-5939; E-mail: sckowalczykowski@ucdavis.edu.
[3] The abbreviations used are: DSB, double-strand break; DAPI, 4′,6-diamidino-2-phenylindole; MES, 4-morpholineethanesulfonic acid; SSA, single-stranded annealing; ds, double-stranded; ss, single-stranded; RPA, replication protein A.

homologous recombination pathways that are dependent on the functions of *RAD52*.

EXPERIMENTAL PROCEDURES

Proteins—Rad52 protein was purified as described (23) except that the Superose-12 column was substituted with a Superdex-200 column (GE Healthcare). A plasmid for overexpression of Rad59 protein in *Escherichia coli* was constructed with a V5 epitope and a hexahistidine tag fused to its C terminus. Expression of this fusion protein in yeast complements the methyl methanesulfonate sensitivity of the *rad59* mutant strain LSY836 (34) to the same extent as the untagged Rad59 protein construct (data not shown). Rad59 protein was overexpressed in BLR(DE3) pLysS (Novagen). Cells were resuspended in 5 volumes of lysis buffer (50 mM MES, pH 6.5, 1 M NaCl, 10% glycerol) supplemented with 10 mM imidazole and 1 mM phenylmethylsulfonyl fluoride and lysed using a French press. The lysate was clarified by high-speed centrifugation at 35,000 × g for 30 min at 4 °C in a Beckman Ti-45 rotor and loaded onto a Ni^{2+}-charged chelating Sepharose column. The column was washed with 5–10 column volumes of lysis buffer containing 50 mM and then with the buffer containing 100 mM imidazole. Rad59 protein was eluted with lysis buffer containing 300 mM imidazole. The eluate was dialyzed twice against 1-liter of MDEG buffer (25 mM MES, pH 6.5, 1 mM dithiothreitol, 1 mM EDTA, 10% glycerol) containing 200 mM NaCl for a period of at least 2 h. The dialysate was spun at 10,000 × g for 1 h at 4 °C in a Beckman JA-20 rotor to remove any precipitate, diluted 3-fold with MDEG buffer, and then loaded onto a 1-ml HiTrap Q-Sepharose column. The flow-through from the Q-Sepharose column was applied to a 1-ml HiTrap heparin-Sepharose column and fractionated with a linear gradient of 100–600 mM NaCl in MDEG buffer. Rad59 protein eluted at ~400 mM NaCl and the peak fractions were dialyzed against storage buffer (25 mM Tris-HCl, pH 7.0, 200 mM NaCl, 1 mM EDTA, 1 mM dithiothreitol, and 10% glycerol). The concentration of Rad59 protein was determined using an extinction coefficient of 35,140 M^{-1} cm^{-1} at 280 nm based on its amino acid composition. RPA was purified as described (35). Restriction endonuclease PstI, human SssI methylase, and T4 polynucleotide kinase were purchased from New England Biolabs. S1 nuclease and proteinase K were purchased from U. S. Biochemical Corp. and Roche Applied Science, respectively.

DNA Substrates—For annealing assays, 48-mer oligonucleotides 25 and 26 were prepared and the concentrations were determined as described (20). The sequences for oligonucleotids 25 and 26 are 5′-GCAATTAAGCTCTAAGCCATCCGCAAAAATGACCTCT-TATCAAAAGGA-3′ and 5′-TCCTTTTGATAAGAGGTCATTTT-TGCGGATGGCTTAGAGCTTAATTGC-3′, respectively. To produce annealed dsDNA control substrate, 80 μM of each oligonucleotide was mixed together in 10 mM Tris-HCl, pH 7.5, 10 mM Mg(OAc)$_2$, 1 mM EDTA and heated to 100 °C for 5 min. The reaction mixture was cooled down slowly to room temperature over a period of ~2 h, to produce a product that was >99% duplex. Complementary oligonucleotides 32F and 32R used in the kinetics study encompass the central 32 nucleotides of oligonucleotides 25 and 26, and the sequences are 5′-GCTCTAAGC-CATCCGCAAAAATGACCTCTTAT-3′ and 5′-ATAAGAGGTCA-TTTTTGCGGATGGCTTAGAGC-3′, respectively. Plasmid DNA pBluescript SK(+) was prepared using a Qiagen Maxiprep kit, linearized with PstI, and heat-denatured at 100 °C for 3 min immediately before use. For the S1 nuclease-based annealing assay, the PstI-linearized pBluescript SK(+) was labeled with tritium using SssI methylase and [^{3}H]S-adenosylmethionine (PerkinElmer Life Sciences), and then denatured as described (36). Concentrations for plasmid dsDNA were

determined using an extinction coefficient of 6,500 M^{-1} cm^{-1} at 260 nm and are expressed in nucleotides.

DAPI Fluorescence-based Annealing Assay—DAPI (4′,6-diamidino-2-phenylindole) was purchased from Molecular Probes. Unless otherwise indicated, the DAPI fluorescence-based assays were carried out as described (20), except that a Shimadzu RF5000U spectrofluorimeter was used. The bandwidths for excitation (345 nm) and emission (467 nm) light were set to 3 and 15 nm, respectively. The levels of 0 and 100% DNA annealing were defined as fluorescence increase over background by the ssDNA substrates and the annealed dsDNA product, respectively. The rate of DNA annealing was determined by measuring the slope from the first measurable 10-s interval (10–20 s) after initiation of the reaction.
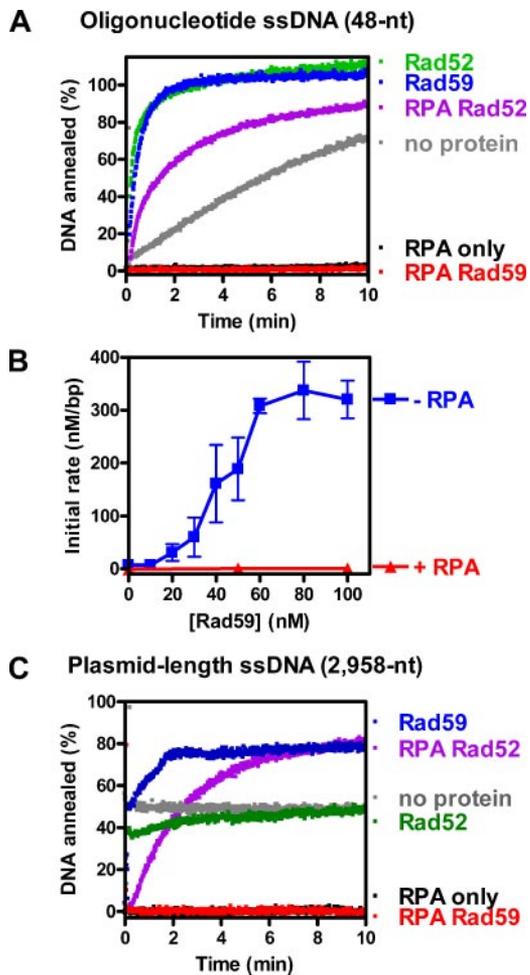
Gel-based DNA Annealing Assay—The annealing reactions contained 1 μM heat-denatured PstI-linearized pBluescript SK(+) DNA in DNA annealing buffer (30 mM Tris-OAc, pH 7.5, 5 mM Mg(OAc)$_2$, 1 mM dithiothreitol). The DNA substrate was first incubated with an excess of RPA (67 nM) or with RPA storage buffer at 30 °C for 5 min. The indicated amounts of Rad52 or Rad59 protein were then added to initiate the reaction. At each time point, a 10-μl aliquot was withdrawn and deproteinized with 1 μl each of 10% SDS and proteinase K (15.3 mg/ml) at 30 °C for 10 min. For the 0-time point sample, SDS/proteinase K was added before addition of Rad52 or Rad59 protein. The annealing products were resolved by 1% agarose gel electrophoresis and quantified using a Storm 840 system and ImageQuant software (GE Healthcare).

S1 Nuclease-based DNA Annealing Assay—The annealing assays were carried out essentially as described above except that 1 μM heat-denatured, tritiated pBluescript SK(+) DNA was used instead. At each indicated time point, a 10-μl aliquot was withdrawn and added to 1 μl of 10% SDS. The mixture was then diluted with 1× S1 reaction buffer (50 mM NaOAc, pH 4.6, 250 mM NaCl, and 1 mM ZnSO$_4$) to a final volume of 150 μl. Heat-denatured calf thymus DNA (2.5 μg; Sigma) and 10 units of S1 nuclease were added to the reaction and the mixture was incubated at 37 °C for 30 min. The nuclease digestion was terminated by addition of 10 μg of heat-denatured calf thymus DNA and an equal volume of cold 10% trichloroacetic acid. The reaction was kept on ice for 30 min and filtered through a GF/C filter (Whatman). Each filter was washed with 1 ml of cold 10% trichloroacetic acid for three times and 1 ml of 95% ethanol once, and air-dried for 10–14 h. The trichloroacetic acid-precipitable radioactivity was measured on a Beckman scintillation counter. The extent of DNA annealing is quantified as the percentage of trichloroacetic acid-precipitable counts relative to the dsDNA control.

RESULTS

Rad52 and Rad59 Anneal Complementary Single-stranded Oligonucleotides in the Absence of RPA—First, we examined the annealing of two complementary oligonucleotides by Rad52 and Rad59 proteins, using a DAPI fluorescence-based method as described previously (20). In the absence of protein, spontaneous annealing resulted in a slow increase of dsDNA-specific DAPI fluorescence over time (Fig. 1*A*, *no protein*). When Rad52 protein was incubated with the first oligonucleotide, addition of the complementary oligonucleotide resulted in an immediate increase in DAPI fluorescence (Fig. 1*A*, *Rad52*). Consistent with the previous report (20), Rad52-promoted DNA annealing was rapid, reaching a plateau in 1–2 min.

Annealing of these oligonucleotides was also accelerated by Rad59 protein. The Rad59-promoted reaction was significantly faster than the spontaneous reaction, and only slightly slower than the Rad52-promoted reaction, reaching a plateau in about 2 min (Fig. 1*A*, *Rad59*). The ability of Rad59 to anneal complementary ssDNA is also consistent with

A Oligonucleotide ssDNA (48-nt)

B

C Plasmid-length ssDNA (2,958-nt)

FIGURE 1. **Rad52- and Rad59-mediated DNA annealing reactions monitored by the DAPI fluorescence-based annealing assay.** *A*, representative time traces for annealing of oligonucleotides. For reactions without RPA, oligonucleotide 25 (200 nM) was incubated with storage buffer, 20 nM Rad52 protein, or 50 nM Rad59 protein as indicated; and the reaction was started by addition of oligonucleotide 26 (200 nM). For reactions containing RPA, the two oligonucleotides were preincubated with 30 nM RPA for 100 s and the reaction was started by addition of Rad52 or Rad59 protein, respectively. *B*, DNA annealing as a function of Rad59 concentration. Reactions were carried out at various Rad59 protein concentrations in the absence (*squares*) or presence (*triangles*) of RPA. Results are averages obtained from at least duplicate experiments and the *error bars* represent the variation in the observed rate. *C*, representative time traces for annealing of plasmid-length ssDNA. Reactions were carried out as described above except the DNA substrate was alkaline-denatured pBluescript SK(+) plasmid DNA (400 nM) with or without preincubation with RPA (30 nM). Reactions were started by addition of Rad52 (20 nM) or Rad59 (50 nM) protein.

previous reports (29, 33). The rate of DNA annealing increased in a sigmoid manner with increasing Rad59 protein concentration (Fig. 1*B*) until a plateau was achieved at about 60–80 nM. The extent of DNA annealing was 100% for Rad59 protein concentrations above 40 nM, but at a lower concentration, the reactions were too slow to determine a reliable end point (data not shown).

Rad52 and Rad59 Anneal Plasmid Length ssDNA in the Absence of RPA—We also examined the annealing activity of Rad59 protein using a longer ssDNA substrate possessing substantial secondary structure: heat-denatured, linearized pBluescript SK(+) DNA (2,958 bases). The secondary structure in plasmid-length ssDNA caused high background fluorescence, at ~50% of the native dsDNA level, and interfered with measurement of DNA annealing. This background signal was stable over the observation time course, however (Fig. 1*C*, *no protein*), indicating no additional spontaneous annealing was occurring. When Rad52 protein was added to the reaction, the DAPI fluorescence signal first

decreased slightly, then gradually increased until it reached the original level, yielding no net increase in fluorescence signal (Fig. 1*C*, *Rad52*). This result is consistent with our previous observation that Rad52 protein alone apparently did not promote measurable annealing of plasmid-length ssDNA due to interference from ssDNA secondary structure (20). In contrast, when Rad59 protein was tested, the fluorescence signal increased, corresponding to annealing of ~30% of the ssDNA (Fig. 1*C*, *Rad59*), consistent with a previous observation that Rad59 protein promotes annealing of plasmid-length ssDNA (33).

Because of the interference from DNA secondary structure in the DAPI assay when plasmid-length DNA was used, we examined DNA duplex formation more directly. The progress of DNA annealing was monitored using agarose gel electrophoresis to separate the ssDNA substrates and annealing products after deproteinization. When heat-denatured plasmid DNA was incubated alone, there was very little DNA annealing that occurred over the 10-min time course (Fig. 2, *A–C, lanes 1* and *2*). In contrast, incubating the ssDNA with Rad52 protein (Fig. 2, *A* and *B, lanes 3–9*) produced an increasing amount of annealed DNA species over time. This result was unexpected because in the DAPI fluorescence-based assay there was little change in dsDNA-specific signal for Rad52 protein. We suspect that, in the DAPI assay, the product-specific fluorescence signal is masked due to interference from the ssDNA secondary structure. In fact, the slight decrease in DAPI fluorescence (~10%) immediately after Rad52 addition (Fig. 1*C*, *Rad52*) suggests that binding of Rad52 to ssDNA may partially disrupt DNA secondary structure. Thus, the decrease in DAPI fluorescence due to reduced secondary structure obscured the fluorescence increase due to DNA annealing.

Similar to Rad52 protein, Rad59 protein annealed the ssDNA and produced slower-migrating DNA species (Fig. 2*C, lanes 4–9*). This result confirmed that Rad59 protein can anneal plasmid-length complementary ssDNA quickly and efficiently as shown in the DAPI assay (Fig. 1*C*) and in a previous report (33).

In the DNA annealing reactions promoted by Rad52 or Rad59 protein, there are two major annealing products: 1) a discrete product that migrates at a position corresponding to unit-length plasmid dsDNA; and 2) a complex product with a slower migration or that fails to enter the gel, indicating the formation of a network structure containing multiple ssDNA molecules. In Rad52-promoted annealing reactions (Fig. 2, *A* and *B*), there were approximately equal amounts of the duplex-length product and the network structure. In contrast, in the Rad59-promoted annealing reaction (Fig. 2*C*), the product was predominantly a DNA network.

Because there was a discrepancy between the DAPI fluorescence- and gel-based annealing assays with respect to the ability of Rad52 to anneal the plasmid-length ssDNA substrates, we used an S1 nuclease-based assay (37) to resolve this inconsistency. Because S1 nuclease degrades ssDNA but not dsDNA, only the annealed dsDNA product will be resistant to S1 nuclease digestion and can be precipitated by trichloroacetic acid (illustrated in Fig. 3). In addition, this assay is better for scoring the extent of annealing in only partially duplex DNA products. Using this assay, we detected Rad52-promoted DNA annealing of long ssDNA (Fig. 3*A*, −*RPA*). Annealing was optimal at 100 nM Rad52 protein, corresponding to 1 Rad52 monomer per 10 nucleotides of ssDNA (Fig. 3*B*). These results are similar to those obtained from the gel-based assay (Fig. 2, *A* and *B*), but are inconsistent with the result obtained from the DAPI assay (Fig. 1*C*). Due to the high interference from the DNA secondary structure in the DAPI assay, we believe that, with plasmid-length ssDNA substrates, results from the gel and S1 nuclease assays are
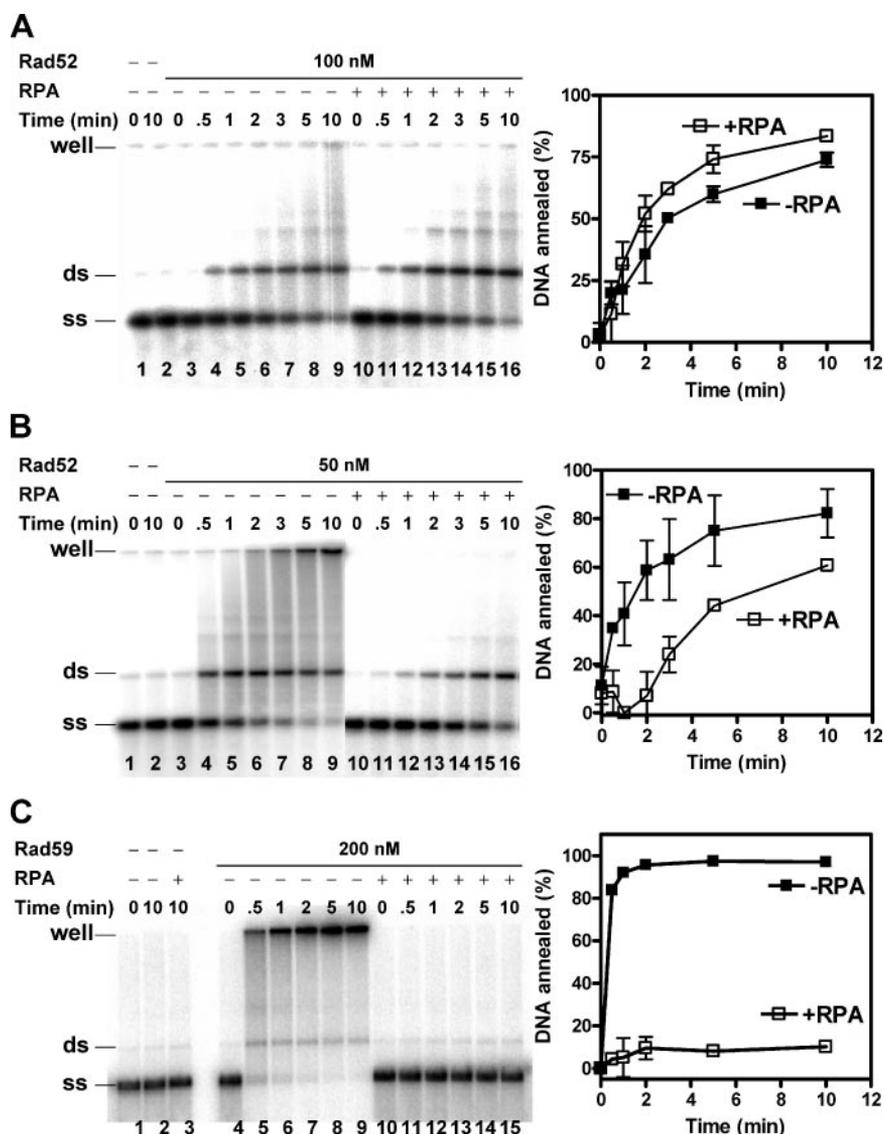
FIGURE 2. **Rad52- and Rad59-mediated DNA annealing monitored by agarose gel electrophoresis.** Reactions were carried out as described under "Experimental Procedures" at a saturating concentration of Rad52 protein (100 nM) (*A*), a subsaturating concentration of Rad52 protein (50 nM) (*B*), and Rad59 protein (200 nM) (*C*), either in the absence (*closed squares*) or presence (*open squares*) of RPA. A representative gel is shown for each reaction in the *left panel*; and the disappearance of ssDNA was quantified and plotted against time in the *right panel*. Results are the average obtained from duplicate reactions and the *error bars* represent the variation in those reactions.

more reliable. Therefore, we conclude that Rad52 protein alone can anneal plasmid-length ssDNA.

Likewise, Rad59 protein promoted annealing of plasmid-length ssDNA as measured by S1 nuclease resistance (Fig. 3*C*). When these results are compared with those from the gel assay (Fig. 2*C*), the yield of apparent annealing is greater in the gel assay than that of dsDNA product formation in S1 nuclease assay. This comparison suggests that Rad59 protein promotes annealing between short stretches of complementary sequences between multiple ssDNA molecules to produce annealing products that are not fully base-paired but that have reduced electrophoretic mobility. The apparent annealing extent measured by the gel assay is faster than that measured by S1 nuclease digestion, further suggesting that additional intramolecular annealing is occurring over time within the initially paired, partially annealed DNA products.

Similar to the annealing of oligonucleotides (Fig. 1*B*, −RPA), DNA annealing of the longer ssDNA showed a sigmoidal dependence on Rad59 protein concentration (Fig. 3*D*, −RPA) suggesting that, under these conditions, at least 1 Rad59 protein per 20 nucleotides is required for DNA annealing. However, at a higher ssDNA concentration, Rad59 protein was reported to promote annealing at a much lower protein to DNA ratio (33). We have also observed DNA annealing by Rad59 protein at ratios as low as 1 protein to 100 nucleotides when the ssDNA

substrate concentration was increased to 40 μM (plasmid-length ssDNA substrate, data not shown). We attribute this variation to the possibility that the affinity of Rad59 for ssDNA is not sufficiently high to confer stoichiometric binding at low DNA concentrations. Consequently, at higher DNA concentrations, protein-DNA complex formation and DNA annealing are more effective.

Unlike Rad52 Protein, Rad59 Protein Cannot Anneal ssDNA That Is Complexed with RPA—A unique feature of Rad52 protein is that it anneals complementary ssDNA complexed with RPA in a species-specific manner (16, 20). Functional homologues of Rad52, the *E. coli* RecO protein (38) and the bacteriophage T4 UvsY protein,[4] can also promote annealing of ssDNA complexed with their cognate single-stranded-binding proteins. In contrast, Rad59 protein was reported unable to anneal plasmid-length ssDNA (33) but was able to anneal short oligonucleotides (29) in the presence of RPA. To examine this potentially unique aspect of DNA annealing more carefully, Rad52- and Rad59-promoted annealing in the presence of a saturating amount of RPA was performed using each of the three different annealing assays described above.

---

[4] N. Kantake, L. Yang, and S. C. Kowalczykowski, unpublished observations.
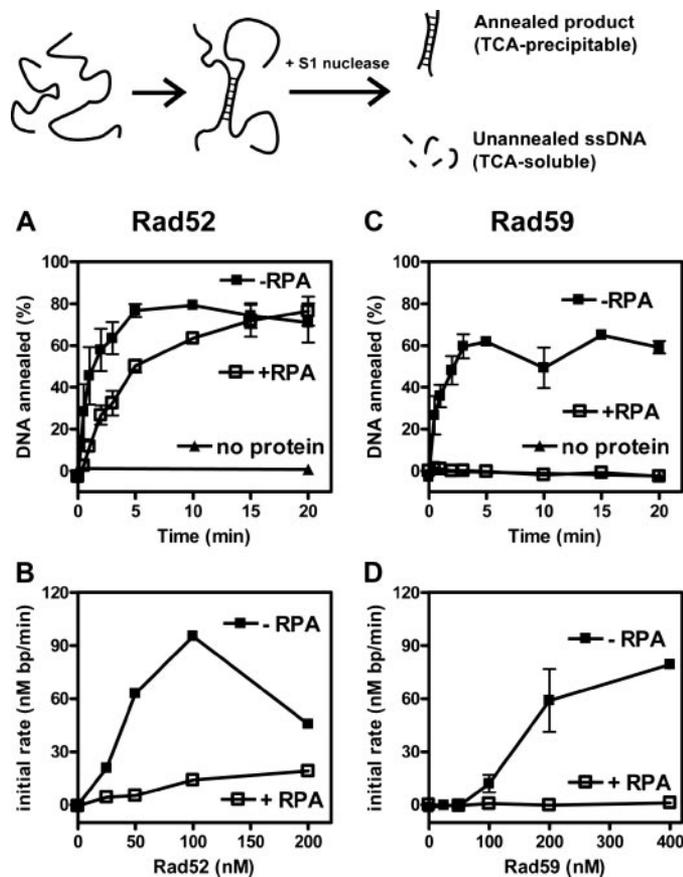
FIGURE 3. **Rad52- and Rad59-mediated DNA annealing monitored by the S1 nuclease-based DNA annealing assay.** A schematic illustration of the S1 nuclease-based DNA annealing assay is shown at the *top* of the figure. *A*, Rad52-mediated DNA annealing. Representative results for DNA annealing promoted by Rad52 protein (100 nM), either in the absence (*closed squares*) or presence (*open squares*) of RPA (67 nM). The spontaneous annealing reaction (*closed triangles*) is included as a control. *B*, the rate of DNA annealing at different Rad52 protein concentrations. Reactions were performed either in the absence (*closed squares*) or presence (*open squares*) of RPA. Results were obtained from a single experiment. *C*, Rad59-mediated DNA annealing. Representative results for DNA annealing promoted by Rad59 protein (200 nM), either in the absence (*closed squares*) or presence (*open squares*) of RPA (67 nM). A spontaneous annealing reaction (*closed triangles*) is included as a control. *D*, the rate of DNA annealing reaction at different Rad59 protein concentrations. Reactions were performed either in the absence (*closed squares*) or presence (*open squares*) of RPA. Results are the average obtained from duplicate experiments and the *error bars* represent the variation in those reactions.

In all three annealing assays, with oligonucleotide and plasmid-length ssDNA substrates, reactions containing only RPA showed no signal increase during the entire time course (Fig. 1, *A* and *C*, *RPA only*; Fig. 2*C*, *lane 3*). Furthermore, in the DAPI assay, the fluorescence signal from the plasmid-length ssDNA decreased to the baseline (Fig. 1*C*, *RPA only*), indicating that RPA not only prevents DNA annealing but, as expected, also removes secondary structure from the DNA.

As previously observed in the DAPI assay (20), Rad52 protein annealed complementary oligonucleotides in the presence of RPA, but at a slower rate (Fig. 1*A*, *RPA Rad52*). Rad52 protein also annealed plasmid-length ssDNA efficiently when RPA was present (Fig. 1*C*, *RPA Rad52*). The gel assay also showed that Rad52 protein could anneal plasmid-length ssDNA complexed with RPA (Fig. 2, *A* and *B*, *lanes 10–16*), consistent with a previous report (16). Interestingly, the presence of RPA favored formation of unit-length duplex DNA, and the amount of network structures was reduced, especially at a suboptimal concentration of Rad52 protein (Fig. 2, *A* and *B*). At 100 nM Rad52 protein, the apparent rate of DNA annealing in the presence of RPA was not much different from that obtained in the absence of RPA in the gel

assay (Fig. 2*A*). At 50 nM Rad52 protein, RPA slowed down annealing in both gel and S1 nuclease assays (Figs. 2*B* and 3*B*). This finding suggests that by removing DNA secondary structure, RPA enhances the ability of Rad52 to fully anneal two ssDNA molecules to form a continuous duplex DNA, rather than to anneal multiple ssDNA molecules into a network structure. The S1 nuclease assay (Fig. 3*A*, +*RPA*) confirms that in the presence of RPA, although the rate of annealing is slowed (Fig. 3, *A* and *B*), the extent of annealing is nearly complete at the base pair level (~80%).

For Rad59 protein, in all three assays, no DNA annealing was detected in the presence of RPA (Figs. 1, 2*C*, and 3*C*). Even when Rad59 protein concentration was increased to a ratio of 1 protein per 2–2.5 nucleotides, there was very little DNA annealing (Figs. 1*B* and 3*D*). Only when the reaction was incubated for a longer period of time (20 min) did a low extent of DNA annealing (~5%) become apparent with the oligonucleotide substrates (data not shown), but not with the plasmid-length ssDNA substrates (Fig. 3*C*). We therefore conclude that Rad59 is unable to promote DNA annealing in the presence of RPA.
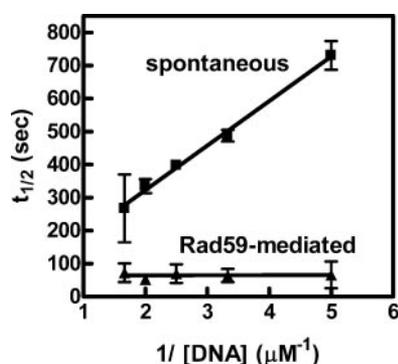
Rad59-promoted DNA Annealing Is a First-order Reaction—The rate of spontaneous DNA annealing is determined by the collision frequency of the two complimentary ssDNA sequences; hence the reaction follows second-order kinetics. It was reported previously that Rad52-dependent DNA annealing follows second-order kinetics, but is 3,500-fold faster than a spontaneous reaction (19). This finding suggested that the rate-limiting step is also determined by the frequency of collision between Rad52-ssDNA and the complementary ssDNA. In contrast, RecA-mediated annealing follows first-order reaction kinetics, indicating that the rate-limiting step is an intermediate step following the encounter of the two ssDNA molecules (39). We examined the reaction kinetics of the Rad59-mediated annealing reaction by measuring the reaction half-time at different ssDNA concentrations. In a plot of the half-time *versus* the reciprocal of initial DNA concentration, a second-order reaction would give a straight line of a slope of $1/k$, where k is the reaction constant, whereas a first-order reaction would yield a horizontal line (with a slope of 0), because the half-time is independent of initial concentration.

To accurately determine the half-time as a function of DNA concentration, we modified the DAPI assay. The 48-nt oligonucleotide substrates are not completely free of potential secondary structure; therefore, we used a shorter pair of oligonucleotides whose sequences are identical to the central 32 nucleotides of the 48-nucleotide oligonucleotide pair used earlier. These oligonucleotides have less predicted secondary structure. To compensate for the poorer binding affinity of Rad59 protein for shorter oligonucleotides, the magnesium ion concentration was lowered to 2.5 mM, which increases the binding affinity of Rad59 protein.[5] As expected, spontaneous annealing of the 32-nucleotide oligonucleotide pair followed second-order kinetic behavior, in that the reaction half-time was a linear function of the reciprocal of initial DNA concentration (Fig. 4, "spontaneous annealing"). The slope is 134.8 ± 11.3 μM/s, which yields an observed reaction rate constant of 7.5×10^3 M^{-1} s^{-1}.

Rad59-mediated annealing behaved differently in that the reaction half-time changed very little for all initial ssDNA concentrations tested (Fig. 4, "Rad59-mediated"). From the average half-time of 65 s, the observed reaction rate constant is 0.011 s^{-1}. We therefore conclude that unlike Rad52-mediated DNA annealing, the Rad59-promoted reaction is a first-order reaction. The fact that Rad59-dependent annealing is first-order suggests there is an additional step following the rapid

---

[5] Y. Wu, unpublished observations.

FIGURE 4. **Rad59-mediated DNA annealing follows first-order reaction kinetics.** Spontaneous (*filled squares*) and Rad59-mediated (*filled triangles*) DNA annealing reactions at different initial DNA concentrations were monitored using the DAPI assay. Reaction half-life was determined and plotted against the reciprocal of initial DNA concentration. Results are the average obtained from two independent experiments, and the *error bar* represents the variation.

encounter of the Rad59-ssDNA complex and complementary ssDNA, during which base pairing occurs and that determines the rate-limiting observed reaction rate.

Rad59 Enhances Rad52-promoted DNA Annealing at Elevated NaCl Concentrations—Both Rad52 and Rad59 protein are important for *RAD51*-independent homologous recombination. Because the functions of *RAD59* depend on those of *RAD52*, and these two proteins interact with each other (29, 32), we tested whether one modulates the biochemical activities of the other. We first examined annealing of the oligonucleotide substrates using the DAPI assay and annealing of the plasmid-length substrates using the S1 nuclease assay, in the absence or presence of RPA. Unfortunately, no significant increase in either annealing rate or annealing extent was observed in these reactions (data not shown). This result contradicts a previous report, in which Rad59 protein was reported to have an additive effect with Rad52 protein in the annealing of RPA-coated ssDNA (29).

Because the importance of Rad59 protein in the SSA pathway increases as the length of homologous sequence decreases (7), we reasoned that the effect of Rad59 on Rad52-mediated DNA annealing might not be obvious at optimal conditions but might be manifest at suboptimal annealing conditions. Because increasing the salt concentration generally reduces the affinity of proteins for nucleic acids, we therefore examined DNA annealing at higher NaCl concentrations using oligonucleotide substrates in the DAPI assay.
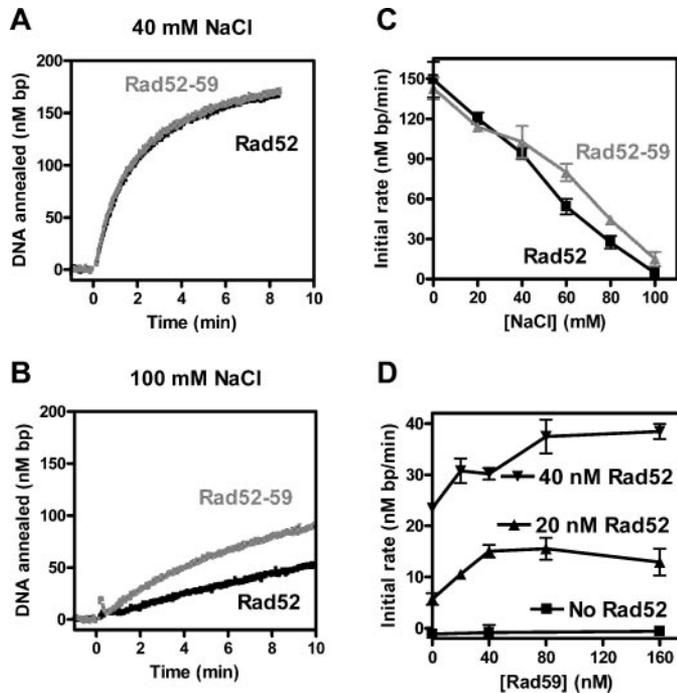
In the absence of RPA, DNA annealing by Rad52 protein was very efficient and no significant decrease in annealing rate or extent was observed at NaCl concentrations of 100 mM or lower. At these conditions, inclusion of Rad59 had no effect, as shown in a representative result obtained at 100 mM NaCl (Fig. 5A). But at 250 mM NaCl, the rate of Rad52-mediated DNA annealing was greatly inhibited (~20 nM bp/min), being only slightly better than the spontaneous rate (~10 nM bp/min). At this condition, inclusion of Rad59 protein resulted in a reaction rate that was about twice as fast (~50 nM bp/min) (Fig. 5B). This enhanced annealing was not due simply to an additive contribution of annealing by Rad59 protein, because at NaCl concentrations of 100 mM and higher, Rad59 protein alone is unable to promote DNA annealing above the spontaneous rate (Fig. 5, *A* and *B*, *Rad59*). The NaCl concentration dependence of DNA annealing promoted by Rad52 protein alone and Rad52-Rad59 proteins combined is shown in Fig. 5C. For both reactions, annealing was gradually inhibited as the NaCl concentration increased, but at NaCl concentrations above ~150 mM, the stimulatory effect of Rad59 becomes evident.

In the presence of RPA, DNA annealing by Rad52 protein was much more sensitive to elevated NaCl concentrations. At 40 mM NaCl, the
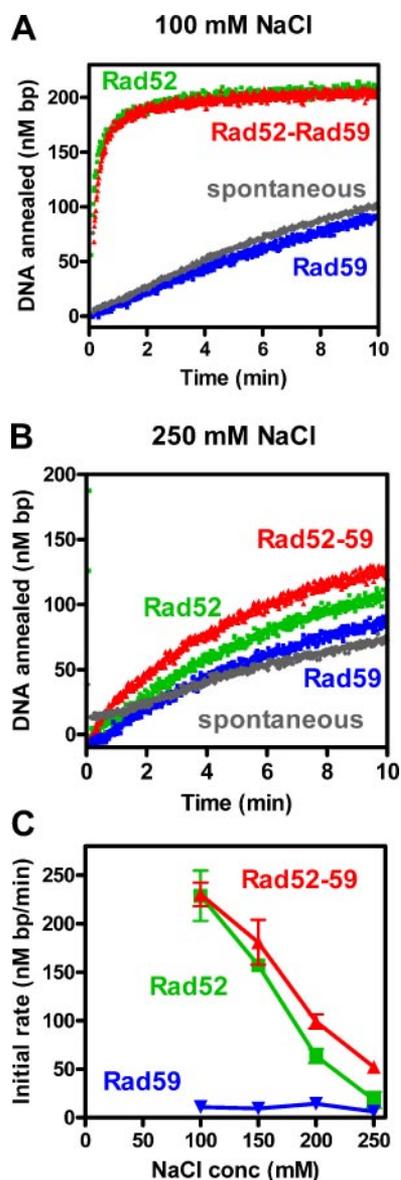
FIGURE 5. **Rad59 protein enhances Rad52-promoted DNA annealing at elevated NaCl concentrations in the absence of RPA.** Annealing of DNA oligonucleotides 25 and 26 was carried out at the indicated NaCl concentration and continuously monitored using the DAPI assay. *A*, representative time traces for DNA annealing reactions in the absence of RPA at 100 mM NaCl in the presence of no added protein (*spontaneous*, *gray*), Rad52 (*green*), Rad59 (*blue*), or Rad52–59 proteins (*red*). Concentrations for Rad52 and Rad59 proteins were 20 and 40 nM, respectively. *B*, representative time traces for DNA annealing reactions in the absence of RPA at 250 mM NaCl, as described in *A*. *C*, initial rates of DNA annealing were calculated and plotted against the NaCl concentration. Results are the average obtained from at least duplicate experiments and the *error bar* represents the variation in the observed rate.

initial rate was reduced by ~50%, and at 100 mM NaCl, DNA annealing was severely suppressed to a rate of ~5 nM bp/min (Fig. 6, *A* and *B*). At NaCl concentrations of 40 mM or lower, there was no significant difference when Rad59 protein was added together with Rad52 protein (Fig. 6C). In contrast, at NaCl concentrations of 60 mM and higher, Rad59 protein stimulated DNA annealing promoted by Rad52 protein. For example, at 100 mM NaCl, a concentration that approaches physiological, the rate for Rad52-Rad59 proteins combined (~10 nM bp/min) was twice as fast as that for Rad52 protein alone (Fig. 6, *B* and *C*). Titration of Rad59 protein at various Rad52 concentrations, but at a fixed DNA concentration, showed that annealing was optimal at Rad59 protein concentrations of 40 and 80 nM when the Rad52 protein concentrations

FIGURE 6. **Rad59 protein enhances Rad52-promoted DNA annealing at elevated NaCl concentrations in the presence of RPA.** Annealing of DNA oligonucleotides 25 and 26 in the presence of 30 nM RPA was carried out at the indicated NaCl concentration and continuously monitored using the DAPI assay. *A*, representative time traces of DNA annealing reactions in the presence of RPA at 40 mM NaCl for Rad52- or Rad52–59-mediated reactions. Concentrations for RPA, Rad52, and Rad59 proteins were 30, 40, and 80 nM, respectively. *B*, representative time traces of DNA annealing reactions in the presence of RPA at 100 mM NaCl for Rad52- (*green*) or Rad52–59- (*red*) mediated reactions as described in *A*. *C*, initial rates of DNA annealing were calculated and plotted against NaCl concentration. Rad52 and Rad59 proteins were co-incubated on ice for at least 15 min before addition. *D*, the effect of Rad59 concentration at no Rad52 (*squares*), 20 nM Rad52 (*triangles*), and 40 nM Rad52 (*inverted triangles*) was examined at 80 mM NaCl. Results are the average obtained from at least duplicate experiments and the *error bar* represents the variation in the observed rate.

were 20 and 40 nM, respectively (Fig. 6*D*). This effect was not due to the ability of Rad59 protein to promote annealing of the RPA-coated ssDNA substrate at increased NaCl concentrations, because there was no DNA annealing in the absence of Rad52 protein (Fig. 6*D*). Thus, optimal stimulation of Rad52-mediated DNA annealing occurs when Rad59 protein is present at a 2:1 stoichiometric ratio with respect to Rad52 protein; because the specific activities of these annealing proteins is not well defined, we cannot say with certainty that this ratio represents the actual molecular ratio of the proteins within the active complex. Nevertheless, these results establish a clear stimulatory function for Rad59 protein in the unique capacity of Rad52 protein to anneal RPA-ssDNA complexes.

DISCUSSION

Both Rad52 and Rad59 Promote DNA Annealing in the Absence of RPA—In this report, we quantitatively analyzed the DNA annealing activity of *S. cerevisiae* Rad52 and Rad59 proteins. In agreement with previous reports (16, 20, 29, 33), we demonstrated that Rad52 and Rad59 proteins promote annealing between complementary ssDNA molecules, using three different assays. Previously, using the DAPI fluorescence-based assay, it was shown that Rad52 protein could mediate annealing of oligonucleotides efficiently, but that the annealing of plasmid-length ssDNA was not detected (20). We re-examined this observation using two additional assays. Although the previous observations from the DAPI assay were reproduced, both the gel and S1 nuclease assays clearly showed that Rad52 protein could anneal plasmid-length

ssDNA in the absence of RPA. Similar to Rad52 protein, Rad59 protein promoted annealing of ssDNA in the absence of RPA. Rad59-dependent DNA annealing is rapid, occurring within a few minutes, and efficient, ranging from 60 to 100% depending on the assay and substrate used. The annealing rates are also comparable with those of another annealing protein, *E. coli* RecO (38).

Rad52-promoted DNA annealing follows second-order kinetics, at a rate ~3500-fold faster than the spontaneous bimolecular reaction (19), indicating that the reaction depends on the frequency of collision between the Rad52-ssDNA complex and complementary ssDNA. From the modeled Rad52-ssDNA complex based on the structure of the human Rad52 N terminus (14), ssDNA is proposed to dock in a positively charged surface of Rad52 protein with the bases pointing outwards from the protein-ssDNA interface. Therefore, the bases are freely accessible to pair with an incoming complementary ssDNA molecule to form dsDNA, consistent with the proposed second-order kinetics.

In contrast to Rad52-mediated DNA annealing, the Rad59-dependent reaction follows first-order kinetics (Fig. 4), which is a characteristic shared with RecA protein (39). The first-order kinetic behavior indicates that the reaction is likely to have at least one intermediate step following the encounter of the Rad59-ssDNA complex with the complementary ssDNA before formation of the dsDNA product. The observed reaction rate would be determined by this rate-limiting unimolecular step, and a minimal kinetic scheme is: ssDNA1-Rad59 + ssDNA2 → [ssDNA1-Rad59-ssDNA2] → [Rad59-dsDNA] → dsDNA + Rad59. Collision of the two ssDNA molecules is the second-order step that must occur at a faster rate compared with subsequent steps. The rate-limiting, first-order step can be either the transition from the Rad59-ssDNA substrate complex to the Rad59-dsDNA product complex, or the dissociation of Rad59 protein from the dsDNA to yield the final product. This difference in reaction order suggests that Rad59 protein may adopt a different ssDNA binding conformation than Rad52 protein.

Rad52, but Not Rad59, Protein Promotes DNA Annealing in the Presence of RPA—We also examined DNA annealing by Rad52 and Rad59 proteins in the presence of RPA. In all of our experiments, we observed that Rad52 promotes DNA annealing in the presence of RPA, but at a reduced rate. Interestingly, when we used a subsaturating concentration of Rad52 protein (relative to the ssDNA), a higher fraction of unit-length plasmid dsDNA product was formed in the presence of RPA, rather than randomly annealed networks of DNA. We have proposed previously (20) that RPA serves an important function in SSA, which is to remove the inhibitory effects of the secondary structure in ssDNA. Our results here demonstrate further the importance of RPA, that RPA facilitates formation of an ordered duplex DNA product with contiguous base pairing between two DNA strands, rather than random DNA networks involving multiple strands.

To date, Rad52 protein is the only protein discovered in *S. cerevisiae* that can anneal complementary ssDNA in the presence of RPA. Rad52 protein binds to RPA (16) and forms a stable co-complex with RPA-ssDNA (25). Because Rad52 protein does not displace RPA from the ssDNA, DNA pairing must occur without first dissociating the RPA-ssDNA complex. Indeed, Rad52-mediated DNA annealing in the presence of RPA follows slower reaction kinetics (Figs. 1 and 3) and is more sensitive to increased NaCl concentrations compared with the reaction without RPA (Figs. 5*C* and 6*C*). At 100 mM NaCl, Rad52-mediated DNA annealing on RPA-coated ssDNA is severely impaired; whereas Rad52-mediated annealing on naked ssDNA is unaffected, indicating that the Rad52-ssDNA complex is stable at 100 mM NaCl. RPA has a high affinity for ssDNA ($K_d \sim 10^{-9}$ M) and the binding of RPA to ssDNA is stable at 0.4 M NaCl (35). Also, the interaction between RPA and Rad52 protein can be detected at NaCl concentrations up to 2 M

Rad59 Protein Is a Rad52 Paralogue

NaCl (40). Therefore, the inability of Rad52 protein to promote annealing of RPA-coated ssDNA at ~100 mM NaCl is not due to the reduced interaction between any two of Rad52 protein, RPA, and ssDNA. Instead, our experiments suggest that, in the presence of RPA, there is an additional intermediate step that is highly sensitive to increased NaCl concentrations. For example, RPA binding to ssDNA involves stacking interactions with the bases (41). For DNA annealing to occur, it is likely that RPA needs to undergo a conformational change, presumably induced by Rad52 protein, to free the bases to permit pairing with a complementary strand. Consistent with this idea, Rad52-mediated annealing of ssDNA coated by RPA-t11, an RPA mutant that is displaced more slowly from ssDNA (35), is even more sensitive to increased NaCl concentrations than the wild-type RPA.[6]

The most prominent difference between Rad52 and Rad59 proteins is their response to RPA-coated ssDNA. Using three independent methods, we find that Rad59 protein does not promote any detectable DNA annealing of RPA-coated ssDNA, regardless of whether the ssDNA is oligonucleotide or plasmid-sized. Our observation is different from a previous report (29). We believe that this difference is likely because of an insufficient amount of RPA used in the previous study: in that report, significant spontaneous annealing occurred in the "RPA alone" control reaction (about 20% at 8 min), suggesting that only a subsaturating amount of active RPA was present in the reaction. In our experiments, the ssDNA substrates remained unannealed during the entire time course of our experiments (Fig. 1–3, *RPA* traces). Therefore, we believe that when RPA is subsaturating, Rad59 protein anneals free ssDNA, but not RPA-ssDNA complexes.

Rad59 Protein Stimulates Rad52-promoted DNA Annealing Under Suboptimal Conditions—Genetic evidence indicates that both *RAD52* and *RAD59* are important in the SSA pathway at the DNA annealing step. Our results support that view, and they further suggest that the two proteins play different roles in the process. When a DSB is processed into ssDNA tails *in vivo*, RPA is the first to bind, given both its rapid kinetics of binding and high affinity for ssDNA. Therefore, an annealing reaction *in vivo* likely always involves a complex of RPA and ssDNA. Rad52, but not Rad59, protein can anneal such an RPA-ssDNA complex. Consequently, this step clearly must be mediated by Rad52 protein. The inability of Rad59 protein to promote annealing of RPA-coated ssDNA suggests that Rad59 does not participate directly in the DNA annealing step *in vivo*. Instead, because Rad52-mediated DNA annealing is optimally enhanced by a stoichiometric amount of Rad59 protein at increased NaCl concentrations, we propose that the function of Rad59 protein is to augment the RPA-ssDNA annealing function of Rad52 protein at physiological (*i.e.* suboptimal) conditions. A previous report showed that Rad52 and Rad59 proteins have an additive effect in DNA annealing at low NaCl conditions (29). We believe this inconsistency is again because of the previously mentioned explanation: *i.e.* that a subsaturating amount of RPA was used in those experiments. Thus, we conclude that a co-complex of Rad52 and Rad59 proteins, at an apparent molar ratio of 1:2, is the functional species responsible for DNA annealing in wild-type cells.

We also believe that our observations, showing Rad59-facilitated DNA annealing by Rad52 protein at increased NaCl concentrations, have biological significance. *In vivo*, the free Na^+ and K^+ concentrations are at least 0.1–0.2 and 0.3 molal, respectively (42). Thus, as shown by genetic studies, SSA is reduced but not eliminated by *rad59* mutations. In addition, genetic studies showed that the dependence of SSA on *RAD59* increases as the length of sequence homology shortens (7), and also that loss of *RAD59* shows a greater reduction in homeologous

recombination than in homologous recombination (43). Our biochemical studies suggest that augmentation of *RAD52* function by *RAD59* might also be important under these suboptimal conditions *in vivo*, such as those encountered during the annealing of imperfect or shorter, less stable complementary sequences.

Rad59 Functions as a Rad52 Paralogue—In summary, it is evident that Rad59 protein, a Rad52 protein homologue, is a DNA annealing protein. But despite the sequence and genetic conservation between Rad52 and Rad59 proteins, their biochemical activities differ in many significant ways. Both the lack of identical activities and the fact that homologous recombination in *rad59Δ* cells is only partially impaired, show that Rad59 protein cannot be viewed as a redundant Rad52 protein. Moreover, Rad59 protein sequences from different fungal species are more similar to each other than to Rad52 protein sequences from the same species, and many invariant residues that are important for the functions of the Rad52 protein *in vivo* are not conserved in the Rad59 protein. Furthermore, when a conserved residue of *RAD52* is changed to one found in the equivalent position in *RAD59*, such as the *rad52-R70K* or the *rad52-L89F* mutants (31), defects in homologous recombination result. Therefore, we propose that Rad59 protein is a Rad52 paralogue, and is the result of an evolutionarily independent lineage. The Rad59 protein manifests unique functions that serve an accessory role for Rad52 protein. This role is analogous to the relationship between the Rad51 protein and the Rad51 paralogues: for Rad51 protein to fully function, it requires assistance from the Rad51 paralogues. Different species have different numbers of Rad51 paralogues and the importance of the Rad51 paralogues varies among different species. In higher eukaryotes, a Rad59-like protein has not yet been identified, despite having an SSA pathway that is surprisingly similar to the one in *S. cerevisiae* (44). However, the *RAD51*-independent pathway has not yet been thoroughly studied, and the existence of an as yet unidentified Rad52 paralogue important to SSA in higher eukaryotes remains a possibility.

REFERENCES

1. Rudin, N., and Haber, J. E. (1988) *Mol. Cell. Biol.* **8,** 3918–3928
2. Paques, F., and Haber, J. E. (1999) *Microbiol. Mol. Biol. Rev.* **63,** 349–404
3. Prado, F., Cortes-Ledesma, F., Huertas, P., and Aguilera, A. (2003) *Curr. Genet.* **42,** 185–198
4. Symington, L. S. (2002) *Microbiol. Mol. Biol. Rev.* **66,** 630–670
5. Bianco, P. R., and Kowalczykowski, S. C. (2002) pp. 46–54, in *Encyclopedia of Life Sciences*, Nature Publishing Group, London
6. Ivanov, E. L., Sugawara, N., Fishman-Lobell, J., and Haber, J. E. (1996) *Genetics* **142,** 693–704
7. Sugawara, N., Ira, G., and Haber, J. E. (2000) *Mol. Cell. Biol.* **20,** 5300–5309
8. Signon, L., Malkova, A., Naylor, M. L., Klein, H., and Haber, J. E. (2001) *Mol. Cell. Biol.* **21,** 2048–2056
9. Sugawara, N., Paques, F., Colaiacovo, M., and Haber, J. E. (1997) *Proc. Natl. Acad. Sci. U. S. A.* **94,** 9214–9219
10. Ivanov, E. L., and Haber, J. E. (1995) *Mol. Cell. Biol.* **15,** 2245–2251
11. Wu, X., Wu, C., and Haber, J. E. (1997) *Genetics* **147,** 399–407
12. Milne, G. T., and Weaver, D. T. (1993) *Genes Dev.* **7,** 1755–1765
13. Ogawa, T., Shinohara, A., and Ikeya, T. (1995) *Adv. Biophys.* **31,** 93–100
14. Singleton, M. R., Wentzell, L. M., Liu, Y., West, S. C., and Wigley, D. B. (2002) *Proc. Natl. Acad. Sci. U. S. A.* **99,** 13492–13497
15. Kagawa, W., Kurumizaka, H., Ishitani, R., Fukai, S., Nureki, O., Shibata, T., and Yokoyama, S. (2002) *Mol. Cell* **10,** 359–371
16. Shinohara, A., Shinohara, M., Ohta, T., Matsuda, S., and Ogawa, T. (1998) *Genes Cells* **3,** 145–156

---

[6] Y. Wu, T. Sugiyama, and S. C. Kowalczykowski, unpublished observations.

17. Van Dyck, E., Hajibagheri, N. M., Stasiak, A., and West, S. C. (1998) *J. Mol. Biol.* **284,** 1027–1038
18. Reddy, G., Golub, E. I., and Radding, C. M. (1997) *Mutat. Res.* **377,** 53–59
19. Mortensen, U. H., Bendixen, C., Sunjevaric, I., and Rothstein, R. (1996) *Proc. Natl. Acad. Sci. U. S. A.* **93,** 10729–10734
20. Sugiyama, T., New, J. H., and Kowalczykowski, S. C. (1998) *Proc. Natl. Acad. Sci. U. S. A.* **95,** 6049–6054
21. Sung, P. (1997) *J. Biol. Chem.* **272,** 28194–28197
22. Shinohara, A., and Ogawa, T. (1998) *Nature* **391,** 404–407
23. New, J. H., Sugiyama, T., Zaitseva, E., and Kowalczykowski, S. C. (1998) *Nature* **391,** 407–410
24. Song, B., and Sung, P. (2000) *J. Biol. Chem.* **275,** 15895–15904
25. Sugiyama, T., and Kowalczykowski, S. C. (2002) *J. Biol. Chem.* **277,** 31663–31672
26. Bai, Y., and Symington, L. S. (1996) *Genes Dev.* **10,** 2025–2037
27. van den Bosch, M., Zonneveld, J. B., Lohman, P. H., and Pastink, A. (2001) *Curr. Genet.* **39,** 305–310
28. Ira, G., and Haber, J. E. (2002) *Mol. Cell. Biol.* **22,** 6384–6392
29. Davis, A. P., and Symington, L. S. (2001) *Genetics* **159,** 515–525
30. Jablonovich, Z., Liefshitz, B., Steinlauf, R., and Kupiec, M. (1999) *Curr. Genet.* **36,** 13–20
31. Bai, Y., Davis, A. P., and Symington, L. S. (1999) *Genetics* **153,** 1117–1130
32. Davis, A. P., and Symington, L. S. (2003) *DNA Repair* **2,** 1127–1134
33. Petukhova, G., Stratton, S. A., and Sung, P. (1999) *J. Biol. Chem.* **274,** 33839–33842
34. Bartsch, S., Kang, L. E., and Symington, L. S. (2000) *Mol. Cell. Biol.* **20,** 1194–1205
35. Kantake, N., Sugiyama, T., Kolodner, R. D., and Kowalczykowski, S. C. (2003) *J. Biol. Chem.* **278,** 23410–23417
36. Steffen, S. E., and Bryant, F. R. (1999) *J. Biol. Chem.* **274,** 25990–25994
37. Bryant, F. R., and Lehman, I. R. (1985) *Proc. Natl. Acad. Sci. U. S. A.* **82,** 297–301
38. Kantake, N., Madiraju, M. V., Sugiyama, T., and Kowalczykowski, S. C. (2002) *Proc. Natl. Acad. Sci. U. S. A.* **99,** 15327–15332
39. McEntee, K. (1985) *Biochemistry* **24,** 4345–4351
40. Kantake, N. (2001) *Mechanism of Homologous Recombination through Studies of DNA Strand Exchange, Recombination Mediator/Annealing and ssDNA Binding Protein.* Ph.D. thesis, University of California, Davis, CA
41. Bochkarev, A., Pfuetzner, R. A., Edwards, A. M., and Frappier, L. (1997) *Nature* **385,** 176–181
42. Olz, R., Larsson, K., Adler, L., and Gustafsson, L. (1993) *J. Bacteriol.* **175,** 2205–2213
43. Spell, R. M., and Jinks-Robertson, S. (2003) *Genetics* **165,** 1733–1744
44. Perez, C., Guyot, V., Cabaniols, J. P., Gouble, A., Micheaux, B., Smith, J., Leduc, S., Paques, F., and Duchateau, P. (2005) *BioTechniques* **39,** 109–115